All-Wheel Drive Electric Vehicle Performance Optimization: From Modelling to Subjective Evaluation on a Static Simulator

All-Wheel Drive Electric Vehicle Performance Optimization: From Modelling to Subjective Evaluation on a Static Simulator

Alessandro Ferraris
Department of Mechanical and Aerospace Engineering
Politecnico di Torino
Torino, Italy
0000-0003-0712-3399

Henrique de Carvalho Pinheiro
Department of Mechanical and Aerospace Engineering
Politecnico di Torino
Torino, Italy
0000-0001-8116-336X

Edoardo Galanzino
Department of Mechanical and Aerospace Engineering
Politecnico di Torino
Torino, Italy

Andrea Giancarlo Airale
Department of Mechanical and Aerospace Engineering
Politecnico di Torino
Torino, Italy
0000-0002-6857-1008

Massimiliana Carello
Department of Mechanical and Aerospace Engineering
Politecnico di Torino
Torino, Italy
0000-0003-2322-0340

***Abstract* — Powertrain electrification is undoubtedly recognized as a major trend in the automotive industry. The elimination of the internal combustion engine opens to different vehicle's architecture designs, to improve habitability and reduce cost. The paper focus on an All-Wheel-Drive Full Electric high-performance vehicle equipped with wheel-hub motors, a layout that offers a significant potential in controlling each wheel individually. The objective is to develop a control algorithm capable of handling wheels torques independently to enhance vehicle's dynamic, keeping into consideration the model's energy performance. The control algorithm is entirely developed in Matlab-Simulink and implemented in the vehicle dynamic model, in a co-simulation environment with VI-CarRealTime software. Offline simulations are performed to tune the controllers and evaluate their impact on vehicle dynamics and energy efficiency. Finally, the model is tested in a real static simulator to be validated and to have a subjective interpretation of the dynamic behavior of the vehicle. Handling improvements are evaluated through a racetrack lap time performed by the VI-Grade virtual driver. Energy efficiency protocols instead will be assessed by monitoring the battery State of Charge variation and their impact on vehicle's behavior will be analyzed on the static simulator. The results point out to an improvement in the lap time thanks to the more agile and less understeering vehicle. Energy optimization algorithms and regenerative braking displays a promising energy reduction without compromising vehicle dynamics. The same racetrack from the offline simulations is used to test the model on the static simulator. Torque vectoring impact on driver's feeling is found to be noticeable and helpful in improving vehicle's response during cornering while energy optimization protocols are not affecting the dynamic performance.**

Keywords — Vehicle Dynamics, Electric Vehicles, Energy Efficiency, Control Strategies, Driving Simulator, Battery Control.

I. INTRODUCTION

Pure battery [1]-[3], hybridization [4]-[6], fuel cells [7], [8] alternative fuels and thermal propulsion systems (ICEs) are all likely to power vehicles to 2040 [9]. However, electrification is undoubtedly recognized as the overarching technology that links them all. For Electric Vehicles (EVs), motors, transmissions and associated controls will need to be integrated to achieve truly miniaturized, efficient packaging to reduce costs and enhance through-life efficiency and maintainability [9]. In-wheel motors have big potential to create an advanced all-wheel drive system for a full electric vehicle that allows additional space for passenger, cargo and battery pack [11].

The increased complexity of the software to control each motor might be seen also as an opportunity to act directly on vehicle dynamics with a simplified powertrain from the mechanical point of view. This paper develops in this direction: exploiting the advantage to directly control each wheel to increase the dynamic and energetic performance of the vehicle. In-wheel motors have not succeeded yet in the automotive industry due to some reluctance shown by manufacturers. The main concern is caused by the increased unsprung mass. A vehicle powered by in-wheel electric motors have a significant greater unsprung mass because the mass of a motor is in each powered wheel. Keeping unsprung mass low is fundamental both for lateral dynamics and ride comfort [12].

The most important advantage related to wheel-hub motors, which also represents the main reason why this EV layout was chosen for this paper, is the possibility to deliver precisely controlled braking or motoring torque on a millisecond timescale [10]. If properly applied, this might lead to great improvements in traction and stability control, reducing stopping distances and enhancing.

Torque Vectoring (TV), for instance, is a major implication related to dynamic stability and performance and, being one major topic discussed in this paper [13].

Starting from a reference vehicle model [14], the goal is the development of an electric powertrain model and a control. Starting from the torque vectoring, all the energy saving algorithms, from

regenerative braking to power efficiency optimization protocol, are introduced simultaneously. This represents the main challenge, as well as the biggest novelty proposed by this paper: harmonize the various goals from energy efficiency and handling, using the capabilities provided by the 4WD electric powertrain. The model was implemented on VI-Grade static simulator to be validated and subjectively evaluated by real drivers.

II. THEORETICAL BACKGROUND

A. Rigid vehicle model

Starting from a rigid vehicle model [14] steady state high speed cornering considers the distribution of cornering forces between the axles and the side slip angles both vehicle and each single wheel, without considering the internal dynamic behavior. The vehicle is to be assumed travelling at constant speed on a curved path with a high radius *R* (much higher than the vehicle's track *t* and wheelbase *l*), with constant speed (*V*), and aerodynamic and self-aligning torques are neglected.

Due to these assumptions, vehicle slip angle β and tires side slip angles α are small; this allows the monotrack (or bicycle) model, schematized in Figure 1 to be used to derive the curvature gain 1/Rδ in Equation (1) and the understeering coefficient K_{us} in Equation (2). The latter is a non-dimensional quantity, usually expressed in rad. It is a fundamental parameter in lateral dynamics, as it represents the understeering behavior of a vehicle.

$$\frac{1}{R\delta} = \frac{1}{l}\frac{1}{1+K_{us}\frac{V^2}{gl}} \qquad (1)$$

$$K_{us} = \frac{mg}{l}\left(\frac{b}{C_1} - \frac{a}{C_2}\right) \qquad (2)$$

where: C_1 and C_2 are the tire coefficients, *m* is the vehicle mass, *a* and *b* are the front and rear axle distances to the center of gravity.

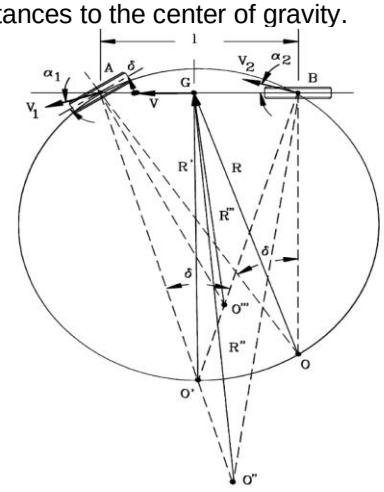

Fig. 1. Side slip angles variation with vehicle lateral behaviour [14]

B. 14 dof model

A vehicle with four wheels can be described by a model with 10 degrees of freedom (DOF) 6 + 2*n* equations of motion where *n* is the number of axles, neglecting the longitudinal slip of the wheels and the compliance of the steering system [14]. If the slips are considered, 14 DOF are necessary. Once the kinematics of the suspensions is defined, it is possible to write the equations of motion. The equations obtained are nonlinear differential equations and its solution can be computed by numerically integrating the equations in time, starting from a given set of initial conditions and specifying the time history of the various inputs [14]. VI-CarRealTime simulation software operates in this way, based indeed on a 14 degrees of freedom model of the vehicle [15]: 6 DOFs from the vehicle sprung mass; 2 DOFs from each wheel, one for describing the motion with respect to the vehicle body and the other the longitudinal slip.

C. Torque Vectoring

The basic working principle of torque vectoring is to distribute torque differently to each single wheel, to generate a yaw moment M_z which contributes to the vehicle cornering. The distribution of the driving force between left and right wheels and, in case of 4WD vehicle with independent motors also between front and rear wheels, allows a better exploitation of the tires' friction limit thus an expansion of the cornering limit [16]. In summary, the main objectives are: Guarantee maximum longitudinal acceleration; Increase lateral dynamic performance in cornering; and Distribute different torques to each electric motor to guarantee maximum energetic efficiency.

To generate yaw moment by means of torque vectoring, a control algorithm needs to be implemented. Since the objective of such control algorithm is to generate a corrective yaw moment M_z, this control technique will be referred to as Direct Yaw Control (DYC) [17]. The control algorithms are mainly based on feedback yaw rate controllers that intervene to track down the error between a reference yaw rate value and the actual yaw rate of the vehicle [18],[19]. The reference yaw rate is outlined in Equation (3).

$$\dot{\psi}_{ref} = r_{ref} = \frac{1}{R\delta}V\delta \qquad (3)$$

where: 1⁄Rδ is the curvature gain, *V* is the vehicle's speed and δ is the wheels' steering angle. *V* and δ are generated by the virtual driver and enter the control system as inputs.

Regarding the actual yaw rate, it is usually computed based on a more complete model of the vehicle, as a 14 DOF model. For this paper, yaw rate DYC was also used, based on a PID feedback control with PID gains depending on vehicle's speed *V*. The PID controller used in the model computes the yaw rate error comparing r_{ref} with the 14 DOF model output.

Beside the feedback yaw rate control, a feedforward control was inserted in the model. This decision was taken to have a continuous reference

yaw moment correction, generated by the feedforward. In this way, the feedback part of the controller, which is responsible for the creation of the precise yaw moment correction, acts in a smoother way because it is based on the reference feedforward signal [18].

Given for granted the dynamic performance advantages related to torque vectoring, this paragraph will focus on the possible implications linked to the energy optimization. In a 4WD full electric vehicle with wheel-hub motor, torques can be independently allocated to each electric motor.

This means that the control algorithm has 4 degrees of freedom to be exploited [20] and 2 DOF have already been used: The first DOF is exploited by the requested longitudinal acceleration, which imposes the total torque to be delivered by the four motors. The second DOF is instead needed for the torque differential imposed by the TV algorithm to generate the required yaw moment M_z. The remaining DOF can therefore be used to have an optimal torque distribution, in order to guarantee an optimal usage of the electric motors from the energetic point of view improving the overall vehicle's efficiency.

III. Vehicle Model and Control Design

The general characteristics of the vehicle considered in this paper are presented in Table I. This data will be used afterwards to build the rigid vehicle model to generate the reference yaw rate signal.

TABLE I. Race Car Characteristics

Parameter	Value
Vehicle sprung mass (m_s)	1052 kg
Vehicle unsprung mass (m_{us})	294 kg
Wheelbase (l)	2713 mm
CG longitudinal front wheel distance (a)	1230 mm
CG height (hg)	381 mm
Track width (t)	1665 mm
Front cornering stiffness (C_{front})	306000 N/rad
Rear cornering stiffness (C_{rear})	348000 N/rad

Taking the CRT vehicle model as a reference, it will be referred to as *input* those parameters entering VI-CarRealTime from Simulink and *output* those exiting CRT and entering Simulink. The chosen motor has a mass of 36 kg directly connected to the wheel hubs, and its able to produce 650 Nm of continuous torque and 1250 Nm of peak torque, as well as 60 kW of continuous power and 80 kW of peak power. Power vs. speed curve and efficiency map is shown in Figure 2.

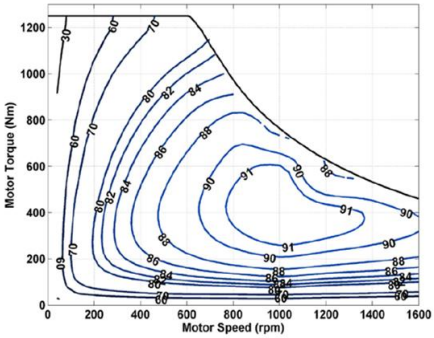

Fig. 2. Torque and Power vs. Speed and Motor efficiency map [21]

The data presented in Figure 2 and the Torque curves also available in [21] are inserted in a properly made Simulink model of the electric powertrain. Being the dynamic response of modern electric motors much faster than wheel dynamics, its influence on vehicle dynamics can be considered not significant [22]. A schematic representation of the control logic flow is displayed in Figure 3.

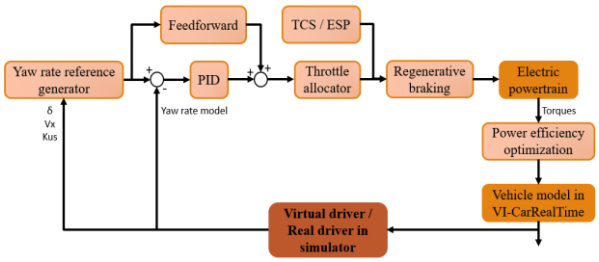

Fig. 3. Control logic flow

Since the controller is working at different velocities, PID gains were chosen not to be fixed but to vary as function of speed. An adaptive PID control algorithm is therefore proposed; gains are updated as function of the speed and, since speed is strictly related to yaw rate, they are also updated as a function of the yaw rate error [18].

IV. Simulation Results and Discussion

A. Ramp steer

Ramp steer manoeuvre was chosen to purely analyse the torque vectoring effects on the vehicle's lateral dynamics in an almost steady state condition. It is an open loop steering manoeuvre, which means that the steering angle is imposed and not controlled by the virtual driver. The driver only controls the throttle demand to assure that the target speed is always maintained. Two ramp steer manoeuvres were created: the first one at constant speed of 90 km/h and a 6 deg/s rate of steering input, while the second is performed at 180 km/h with a lower steering rate of 3 deg/s. Both manoeuvres have a 10 s total duration.

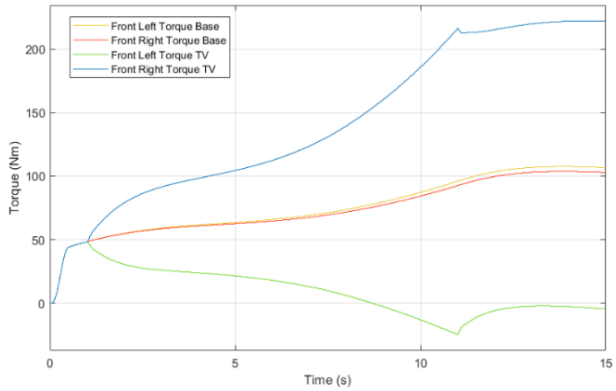

Fig. 4. Front left and front right wheel torques

In the first ramp steer, the vehicle is distant from its limit condition; however, the effects of torque vectoring are already clearly visible. The controller effectively imposes the reference yaw rate to the vehicle and, in order to do that, generates an additional yaw moment applying different torques to the left and right side of the vehicle. As displayed in Figure 4, even negative torques can be requested.

The difference between the base vehicle and the controlled one in terms of understeering gradient is shown in Figure 5. It proves that the controlled vehicle is more responsive than the base one, obtaining a higher lateral acceleration for the same steering wheel angle.

This means that the torque vectoring decreases the understeering behaviour of the vehicle and improves corner entry; this last assumption will be widely analysed during the static simulator tests.

To better highlight the vehicle improved responsiveness, a second ramp steer at higher speed and higher lateral acceleration has been analysed. Without repeating the considerations made on torque allocation and increased yaw rate, the influence of torque vectoring on the understeering gradient are analysed.

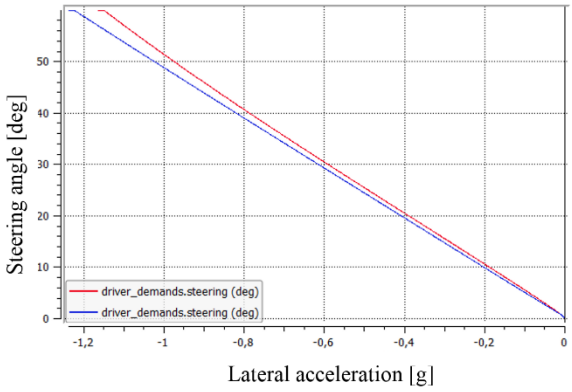

Fig. 5. Wheel steering angle vs. lateral acceleration in the first ramp steer test (red: base, blue: controlled)

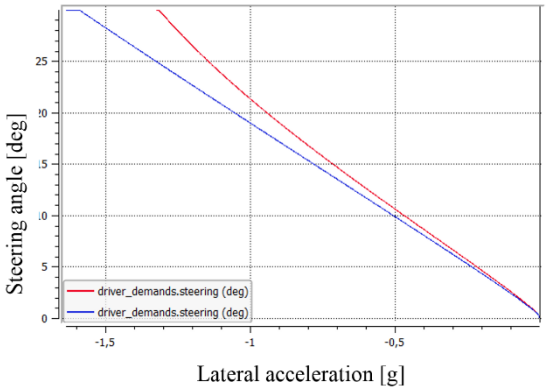

Fig. 6. Wheel steering angle vs. lateral acceleration in the second ramp steer test (red: base, blue: controlled)

Comparing Figure 5 to Figure 6, the increased lateral acceleration of the vehicle better highlights the difference between the base and the controlled one. Above 1g of lateral acceleration, the behaviour of the base vehicle shifts towards a more understeering one. Torque vectoring instead helps in maintaining a linear relationship between the steering input and the lateral acceleration, improving the handling capability. This linear behaviour translates in a constant understeering coefficient.

B. Racetrack

The chosen racetrack is a short version of Hockenheimring that includes high speed and low speed curves, to better judge torque vectoring behaviour, and is approximately 2600 m long. Flying lap time has proven to be a useful tool to evaluate performance gain given by torque vectoring implementation

As shown in Table II, lap time decreased of 0.651 s. This result is to be considered satisfying as it was obtained with the only torque vectoring application, without modifying any characteristic of the vehicle. Hereafter, some relevant plot is reported to better highlight how TV improves lap time.

From now on, the graphs referred to the Racetrack simulation have in abscissa the vehicle's path instead of simulation time, to better compare the two vehicles along the track.

TABLE II. LAP TIME IMPROVEMENT

Driving mode	Lateral PF	Lap Time [s]	Δ Lap Time Base [s]	Δ% Base
Base	1,10	63,271	0	0
With TV	1,16	62,620	-0,651	-1,03

Studying the speed profile of the two vehicles, it is clear how the controlled one has always higher speed when entering a curve (each local minimum in Figure 7).

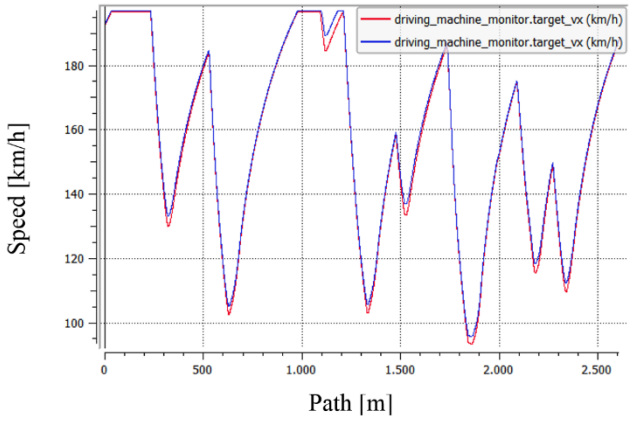

Fig. 7. Speed profile (red: base, blue: controlled)

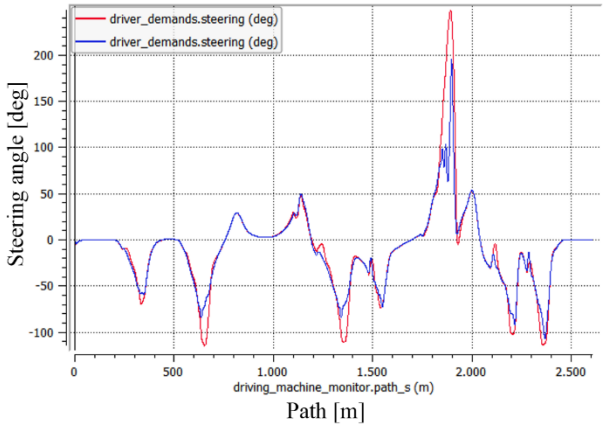

Fig. 8. Steering wheel angle demand (red: base, blue: controlled)

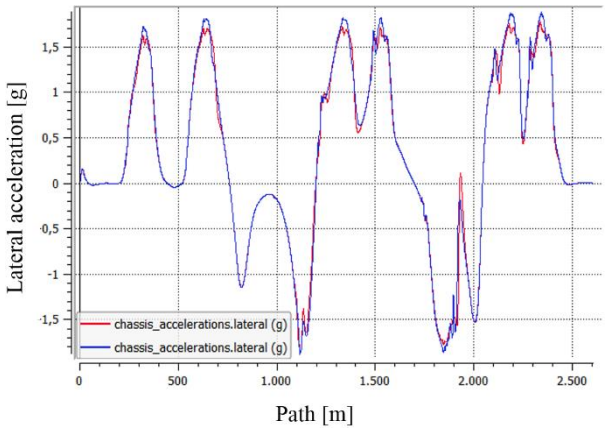

Fig. 9. Vehicle lateral acceleration (red: base, blue: controlled)

Indeed, as explained when discussing the ramp steer results, torque vectoring decreases the understeering behavior and enhances the response of the vehicle. The driver can therefore enter the curve faster, applying a smaller steering angle and gaining higher lateral acceleration, as shown in Figure 8 and Figure 9.

V. Model Validation on Static Simulator

The model was validated on a static driving simulator at VI-Grade head office in Udine. The purposes of the driving session at the simulator mainly consisted in: Full Simulink model validation; Subjective evaluation of the vehicle's behavior depending on the active controller; Comparison between virtual and real driver driving style.

This reveals to be helpful in exploring vehicle's working conditions not always analyzed with a virtual driver. Apart from responsive pedals and steering wheel, the simulator is equipped with an active seat: the belt and the seat itself are used to exert inputs on the driver to simulate the longitudinal and lateral acceleration respectively.

Torque vectoring was tested to subjectively evaluate its effect on vehicle's behaviour and, afterwards, the PID related controller was re-calibrated trying to improve the vehicle's response based on driver's feeling. During the simulator session, the data was logged in Matlab to be then compared with the virtual driver results. First of all, the throttle demand and brake demand of the virtual driver are compared to those of the real driver, to highlight the different driving style.

The real driver approaches the curves at lower speed. This can be noted in Figure 10 where the two speed profiles are compared. The real driver starts braking earlier and its brake demand is completely different from the virtual driver one.

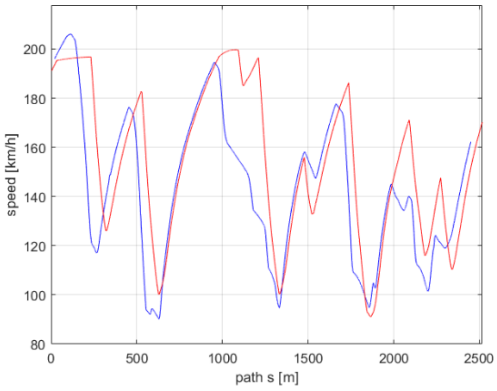

Fig. 10. Speed profiles (red: virtual driver, blue: real driver)

Analyzing the torque vectoring influence on vehicle's behavior, mainly three aspects were noticed: the vehicle is *more oversteering* and therefore reactive when entering a curve; it is more *difficult to predict* when the vehicle is reaching its limit (oversteering); if braking during cornering, torque vectoring *helps in stabilizing* the vehicle avoiding oversteering.

The comparison between the speed profiles and steering wheel demands of the real driver with and without torque vectoring are here reported to support the analysis. Figure 11 highlights the higher speed of the vehicle equipped with torque vectoring when entering a curve.

Apart from the direct effect of torque vectoring on dynamics, the increased performance is also consequence of an improved driver's feeling linked to a more responsive vehicle. The steering angles of the two simulations case, represented in Figure 12, are almost similar; however, considering the higher speed of controlled model during cornering, the resulting

lateral acceleration is higher. As explained during ramp steer, this behavior implies a more oversteering vehicle.

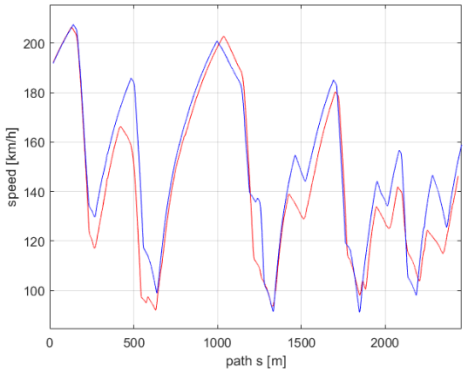

Fig. 11. Speed profiles (red: TV OFF, blue: TV ON)

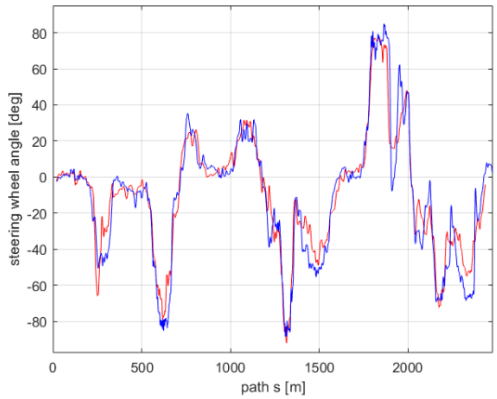

Fig. 12. Steering wheel demand (red: TV OFF, blue: TV ON)

The PID gains related to torque vectoring controller were modified to analyze their influence on vehicle response. The comparison is based on steering wheel angles because, being steering an input to the system, it represents the reaction of the driver to the different vehicle response.

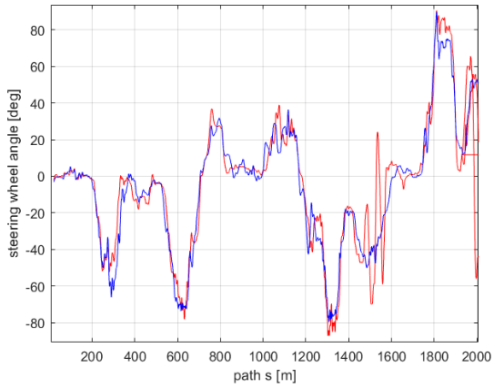

Fig. 13. Steering wheel angle demand (red: high I gain, blue: low I gain)

In Figure 13, two simulations having different torque vectoring proportional and integral gains are compared.

Red line is the proportional gain set to zero and integral gain increased ten times with respect to the original and the blue line the proportional gain increased five times and integral gain kept equal to the original.

Having a too large integral gain resulted in a highly oversteering vehicle with a more invasive but less reactive torque vectoring; the driver therefore sensed the car as extremely unstable during cornering.

In Figure 13 this instability is highlighted at a path between 1400 m and 1600 m during which the driver counter steers to correct vehicle behavior and avoid instability. Energy saving algorithms (regenerative braking, power efficiency optimization and slip reduction algorithms) were tested to subjectively evaluate their effect on driver's feeling. No differences were noticed by the driver in vehicle's behavior neither in acceleration/braking nor during cornering.

VI. CONCLUSIONS

The objective of this paper was to develop an electric powertrain and an innovative control algorithm to highlight the potential of Full Electric Vehicles equipped with in-wheel motors. The performance increase achieved through the controller application was evaluated both from the dynamic and energetic point of view. Starting from the idea of torque vectoring to enhance vehicle dynamics, a more complete control design including also energy optimization protocols was developed. The controller was evaluated based on two maneuvers: Ramp steer to study torque vectoring performance in a standard steady state maneuver; Racetrack lap time to evaluate the interaction between torque vectoring and energy algorithms in a high-performance maneuver. Ramp steer maneuver shows a decreased understeering behavior of the vehicle, and a linear relationship between steering angle and lateral acceleration up to the adherence limit.

The interaction between the controllers was tested in the racetrack lap. Torque vectoring allowed a reduction in lap time of 0.651 s (approx. 1%). Both regenerative braking and power efficiency optimization protocols decreased vehicle's energy consumption up to 20.9% globally.

The influence of torque vectoring on driver's feeling was clearly noticeable during the driving session on the static simulator. The less understeering vehicle proved to be more agile when entering the curve and the steering response was highly improved. Energy optimization protocols' impact on vehicle's response was also evaluated during the driving session and considered not relevant.

ACKNOWLEDGMENTS

The authors wish to acknowledge VI-grade Italy Team: Alessio, Francesco and all the team helping in the activities.

REFERENCES

[1] Scavuzzo, S., Guerrieri, R., Ferraris, A., Airale, A.G. and Carello, M., "Alternative Efficiency Test Protocol for Lithium-ion Battery". International Conference on Environment and

Electrical Engineering and 2018 IEEE Industrial and Commercial Power Systems Europe, EEEIC/I. Palermo, 12-15 June (2018), DOI: 10.1109/EEEIC.2018.8493664.

[2] Cittanti D., Ferraris A., Airale, A.G., Fiorot, S., Scavuzzo S. and Carello M., "Modeling Li-ion batteries for automotive application: A trade-off between accuracy and complexity", International Conference of Electrical and Electronic Technologies for Automotive, Torino 15-16 June 2017, pp. 8, 2017, ISBN: 978-88-87237-26-9, DOI: 10.23919/EETA.2017.7993213.

[3] De Vita A., Maheshwari A., Destro M., Santarelli M. and Carello M., "Transient thermal analysis of a lithium-ion battery pack comparing different cooling solutions for automotive applications", Applied Energy, Vol. 206, pp. 12, 2017, ISSN: 0306-2619, DOI: 10.1016/j.apenergy.2017.08.184.

[4] Cubito, C., Rolando, L., Ferraris, A., Carello, M. and Millo, F., 'Design of the control strategy for a range extended hybrid vehicle by means of dynamic programming optimization'. IEEE Intelligent Vehicles Symposium (IV), Los Angeles, CA, USA 11-14 June, pp. 1234–1241 (2017), ISBN: 978-1-5090-4804-5, DOI: 10.1109/IVS.2017.7995881

[5] Ferraris A., Airale A.G., Messana A., Xu S. and Carello M. 'The regenerative braking for a L7e Range Extender Hybrid Vehicle' International Conference on Environment and Electrical Engineering and 2018 IEEE Industrial and Commercial Power Systems Europe, EEEIC/I. Palermo, 12-15 June (2018), DOI: 10.1109/EEEIC.2018.8494000.

[6] Carello, M., Ferraris, A., Airale, A. and Fuentes, F., 'City Vehicle XAM 2.0: Design and Optimization of its Plug-In E-REV Powertrain'. SAE International Congress, Detroit (Michigan) 8-10 April, pp. 11, (2014), DOI 10.4271/2014-01-1822.

[7] Carello M., De Vita A. and Ferraris A., 'Method for Increasing the Humidity in Polymer Electrolyte Membrane Fuel Cell', Fuel cells, Wiley-Vch Verlag GmbH & Co. KGaA,Weinheim, pp. 8, ISSN: 1615-6854, DOI: 10.1002, 2016.

[8] Ferraris, A.; Messana, A.; Airale, A.G.; Sisca, L.; de Carvalho Pinheiro, H.; Zevola, F. and Carello, M., 'Nafion® Tubing Humidification System for Polymer Electrolyte Membrane Fuel Cells'. Energies 2019, 12, 1773. DOI: 10.3390/en12091773

[9] "Advanced Propulsion Center roadmap." [Online]. Available: https://www.sae.org/news/2018/08/advanced-propulsion-center-future-propulsion-report. [Accessed: 23-Jan-2019].

[10] Hilton A. W. and Hilton C., 'Protean Electric's In-Wheel Motors Could Make EVs More Efficient', IEEE Spectrum: Technology, Engineering, and Science News, 26-Jun-2018. [Online]. Available: spectrum.ieee.org/transportation/advanced-cars/protean-electrics-inwheel-motors-could-make-evs-more-efficient. [Access: 23-10-18].

[11] Wang J., Wang Q., Jin L. and Song C., 'Independent wheel torque control of 4WD electric vehicle for differential drive assisted steering', Mechatronics, vol. 21, no. 1, pp. 63–76, Feb. 2011.

[12] Xu S., Ferraris A., Airale A. G. and Carello M., 'Elasto-kinematics design of an innovative composite material suspension system', Mechanical Sciences, vol. 8, n. 1, pp. 11–22, feb. 2017, DOI: 10.5194/ms-8-11-2017.

[13] Vos R., Besselink I. J. M., and Nijmeijer H., "Influence of in-wheel motors on the ride comfort of electric vehicles," *Proc. 10th Int. Symp. Adv. Veh. Control AVEC10 22-26 August 2010 Loughb. U. K.*, pp. 835–840, 2010.

[14] Genta G. and Morello L., 'The automotive chassis'. Dordrecht: Springer, 2009.

[15] "VI-CarRealTime 17.1 Documentation," p. 887, 2016.

[16] Sawase K. and Ushiroda Y., 'Improvement of Vehicle Dynamics by Right-and-Left Torque Vectoring System in Various Drivetrainsx', Mitsubishi Motors Technical Review, p. 7, 2008.

[17] Fu C., 'Direct Yaw Moment Control for Electric Vehicles with Independent Motors', p. 176.

[18] Novellis L. D., Sorniotti A., Gruber P., and Pennycott A., 'Comparison of Feedback Control Techniques for Torque-Vectoring Control of Fully Electric Vehicles', IEEE Trans. Veh. Technol., vol. 63, no. 8, pp. 3612–3623, Oct. 2014.

[19] De Novellis L., Sorniotti A., Gruber P., Shead L., Ivanov V., and Hoepping K., 'Torque Vectoring for Electric Vehicles with Individually Controlled Motors: State-of-the-Art and Future Developments', World Electr. Veh. J., vol. 5, no. 2, pp. 617–628, Jun. 2012.

[20] Wong A., Kasinathan D., Khajepour A., Chen S.-K., and Litkouhi B., 'Integrated torque vectoring and power management framework for electric vehicles', Control Eng. Pract., vol. 48, pp. 22–36, Mar. 2016.

[21] "ProteanDrive," *Protean*. [Online]. Available: https://www.proteanelectric.com/protean-drive/. [Access: 23-02-19].

[22] Tahami F., Kazemi R., Farhanghi S., and Samadi B., 'Fuzzy Based Stability Enhancement System for a Four-Motor-Wheel Electric Vehicle', SAE Automotive Dynamics & Stability Conference and Exhibition, 2002